Biophysical*Journal*
Article

Biophysical Society

Thermal inactivation scaling applied for SARS-CoV-2

Shahar Seifer[1,*] and Michael Elbaum[1]
[1]Chemical and Biological Physics, Weizmann Institute of Science, Rehovot, Israel

ABSTRACT Based on a model of protein denaturation rate limited by an entropy-related barrier, we derive a simple formula for virus inactivation time as a function of temperature. Loss of protein structure is described by two reaction coordinates: conformational disorder of the polymer and wetting by the solvent. These establish a competition between conformational entropy and hydrophobic interaction favoring random coil or globular states, respectively. Based on the Landau theory of phase transition, the resulting free energy barrier is found to decrease linearly with the temperature difference $T - T_m$, and the inactivation rate should scale as U to the power of $T - T_m$. This form recalls an accepted model of thermal damage to cells in hyperthermia. For SARS-CoV-2 the value of U in Celsius units is found to be 1.32. Although the fitting of the model to measured data is practically indistinguishable from Arrhenius law with an activation energy, the entropy barrier mechanism is more suitable and could explain the pronounced sensitivity of SARS-CoV-2 to thermal damage. Accordingly, we predict the efficacy of mild fever over a period of $\sim$24 h in inactivating the virus.

SIGNIFICANCE We derive a prediction for thermal inactivation of virus by protein denaturation. The model is based on the Landau theory of second-order phase transitions with an entropy-related barrier. Fits to measurements of inactivation of coronaviruses are as successful as the conventional Arrhenius model but with a clear thermodynamic justification and more reasonable span of parameters. The predicted temperature dependence of inactivation times will be useful for combatting the Covid-19 pandemic in the face of limited available data.

INTRODUCTION

Thermal inactivation is an important mechanism for decontamination of viral pathogens, including the novel coronavirus severe acute respiratory syndrome coronavirus 2 (SARS-CoV-2). Relevant contexts include decontamination of surfaces, proposed thermal treatments such as heated ventilation, the possible influence of summer weather, and fever as a physiological response. Indeed, moderate fever, defined as body temperatures between 38.3 and 39.4°C, is lately considered a favorable response of the body against SARS-CoV-2 (1). Fever has been associated with improved survival rates during typical complications (2) and may be significant at early stages of infection as well. Coronaviruses are particularly prone to heat damage. Both the membrane proteins (3–5) and nucleocapsid protein (6) are easily affected by heat.

Experimental studies of thermal inactivation have tabulated results for a number of coronavirus types. One aim has been to clarify safe protocols for decontamination of shared instruments or personal protective equipment (7). Another is to extrapolate an inactivation time from measurements at high temperature to more modest temperatures. A number of heuristic models have been suggested as a basis for fitting the data (8). The Arrhenius equation for a thermally activated process is seemingly attractive as a physical model and was used by two groups to extrapolate from isolated measurements to a continuous temperature variable (9,10). The treatments remain phenomenological, however, so the extracted parameters cannot properly be assigned a physical interpretation. Most importantly, the activation barrier is a free energy with an entropic contribution rather than a fixed energy.

We propose that the scaling in time of a rate-limited process of irreversible virus inactivation should be described instead as a second-order, entropy-driven phase transition,

---

Submitted August 28, 2020, and accepted for publication November 23, 2020.

*Correspondence: shahar.seifer@weizmann.ac.il

Editor: Anatoly Kolomeisky.
https://doi.org/10.1016/j.bpj.2020.11.2259

© 2020 Biophysical Society.

consistent with the coil-globule transition in protein dynamics (11–13). On this basis, we derive a simpler formula relating the inactivation rate to temperature with two fitting parameters that can be determined from data available in the literature. Together with new data (5,14) available on SARS-CoV-2 hosted in cell cultures, we can predict the period in which moderate fever is effective against the virus. During the course of illness, the patient may be exposed to repeated infections from viral residues; hence, it is important to know the significant duration of one fever episode.

METHODS

Model

Although we do not know the mechanism of the virus inactivation in detail, we can approach the problem of thermal damage from a biophysical perspective. RNA is stable at moderate temperatures (5), so one expects loss of protein function. In general, protein inactivation may arise from various mechanisms, including hydrolysis, oxidation, aggregation, kinetically trapped conformations, and denaturation by unfolding (15). Moderate heating is known to cause irreversible inactivation of membrane proteins on the SARS viruses (3,4), as well as the nucleocapsid protein N (6). The incipient process of inactivation at temperatures so close to physiological is expected to involve a conformational rather than chemical modification. In particular, we consider the exposure of hydrophobic regions to the solvent as a plausible root of inactivation (16,17). The question considered is how temperature affects the rate of inactivation.

As a concrete example, we consider the globule-coil transition in proteins as a critical path in the inactivation process. Coronaviruses are characterized by elaborate spike proteins protruding from the membrane (18), the denaturation of which would prevent interactions with cellular receptors that are essential for infection. Loss of protein structure is often considered in two steps (11,13): first, the melting of order in the globular domains, and then expansion to a random coil. The melting stage has been identified as a first-order phase transition (11), which has been attributed to vibrational states (19). The second stage involves a second-order phase transition related to conformational entropy of the polymer (12,19), balanced by intramolecular interactions (20).

The kinetics of a multistage process depends primarily on the rate-limiting step, the origin of which may be either an activation energy barrier or a geometric obstruction, i.e., any spatial constraint affecting entropy. A melting transition is favorable above a certain temperature; the melting rate is normally constrained by thermal diffusion necessary to supply the latent heat. Latent heat is not a relevant activation energy barrier because the free energy does not change along the process. Therefore, the second stage in a globule-coil transition is the rate-limiting process, once allowed.

Should the inactivation process involve disruption of covalent bonds, it would entail an energy barrier E_a that limits the rate of the transition $k(T)$. Such a transition is justly described by the Arrhenius law, $k(T) = A\exp(-E_a/RT)$, with temperature T expressed in absolute Kelvin units and R the gas constant. E_a is presumed to be constant in temperature, and the proportionality factor A represents an attempt frequency with units of inverse time. In the fits of (9), $\ln(A)$ shows a span of 58, meaning that A varies over 25 orders of magnitude only among different types of coronaviruses. A physical range of A that might be expected is at most a few orders of magnitudes, as seen, for example, considering molecular dynamics of alanine peptide in various conformational transformations (21). The linearity demonstrated between $\ln(A)$ and E_a (conforming to the Meyer-Neldel rule) is more likely a manifestation of the finite duration of inactivation time rather than verification of the mechanism. On the other hand, most often the mechanism of inactivation involves denaturation due to structural changes, possibly a transition from a "correctly" folded state located at a minimum in free energy to a random-coil state at another local minimum in free energy (22,23). The bottleneck in such a transition depends on a free energy barrier $\Delta G = \Delta(E - TS)$ between the rest states, where S denotes entropy. Thus, thermal fluctuations provide a certain chance to overcome an internal energy barrier but equally could allow a biological system to transit a temporary decrease in entropy, for example, to resolve entanglement.

A generalized law of transition rates can be stated as $k(T) = A\exp(-\Delta G/RT)$, where $\Delta G = \max_{\eta_0 \le \eta \le \eta_f}\{G(\eta, T)\} - G(\eta_0, T)$, A is the kinetic rate, and η denotes the reaction coordinate. Namely, the free energy barrier ΔG is determined by the initial state η_0 and the intermediate state at which the free energy $G = E(\eta) - S(\eta)T$ is maximal. Zwanzig offered the term entropy barrier (24) to suggest that a reaction could be obstructed by a negative step in entropy $|\Delta S|$. Also according to Zwanzig, a transition obstructed by a purely geometrical bottleneck, for example the passage of a particle through a narrow barrier, could be accelerated according to $exp(S/R)$ by an increase in entropy. The relevant entropy barrier in the case of the globule-coil transition is related to the hydrophobic volume around the internal structure of the polymer (25,26) consisting of hydrophobic groups and narrow gaps that prevent solvent penetration. In effect, the entropy barrier preserves the molten globule stably in a compact state (11,12).

The transition from molten globule to coil can be modeled mathematically as a perturbation dependent on two order parameters. One order parameter is the conformational disorder of the polymer, η_p, which increases with respect to the native fold. According to the Landau theory of second-order phase transitions (27), near a transition temperature T_m, the free energy perturbation depends on the order parameter η_p as $G(\eta_p, T) = a(T - T_m)\eta_p^2 + B\eta_p^4$, with $a < 0$ and $B > 0$, assuming $T > T_m$. Because $G = E - ST$, the change in entropy can be written as $S(\eta_p) = |a|\eta_p^2$ and the change in energy $E(\eta_p) = B\eta_p^4 + |a|T_m\eta_p^2$. Initially, η_p is found at a minimum in free energy: $\eta_{p0}^2 = |a|(T - T_m)/2B$, $G_0 = -a^2(T - T_m)^2/4B$. Thus, the rest state varies with temperature in a reversible way, returning to null perturbation at $T \le T_m$.

This description conforms to the stability of the molten globule, which suggests that the entropic drive of the polymer to coil is balanced by a certain energy that increases with conformational disorder. We identify the order parameter as $\eta_p = \sqrt{N}$, according to N bending points added to the polymer, which becomes more flexible with respect to the native fold. As a perturbation to a particular geometry at equilibrium, i.e., the native fold, the N bending points will raise elastic energy proportionally to N and will raise the entropy proportionally to N according to the number of random walk segments. Similarly, the Landau description can build on Flory theory (20) if we define $\eta_p = \sqrt{-\Delta R/R_0}$, where ΔR is a negative change in the average size of the polymer with respect to R_0, the size at rest in athermal solvent. Progression toward the random coil should decrease the polymer size and increase energy because of shortening distance between repulsive residue groups.

Wetting by the solvent entails another order parameter η_s, which varies between 0 (native hydrophobic configuration) and 1 (fully wet or solvated). Wetting involves rearrangement of both the solvent molecules and the distances between chain segments, which carries an entropy cost $|\Delta S_{solv}|$. In addition, wetting by water suppresses both the hydrophobic interactions (e.g., clustering of hydrophobic amino acid residues) and electrostatic interactions (28). Hence, we assume that $E(\eta_p)$ fully vanishes when the polymer is wet because its long-range repulsive interactions are suppressed. Therefore, the general free energy of the system is found to be

$$G(\eta_p, \eta_s, T) = (1 - \eta_s)E(\eta_p) - \eta_s \Delta S_{solv} T - S(\eta_p)T$$

$\Delta S_{solv} < 0$ is the dominant entropic barrier in the model.

At the microscopic level, a fluctuation that successfully manages to solvate the polymer is of low probability but the action itself should be very rapid, depending on the thermal velocity of water molecules. During a successful action of water penetration, the polymer folding state is relatively static. With this idealization, we consider that the reaction path propagates along a constant η_p, whereas η_s varies from 0 to 1. Hence, the free energy reaches its maximum at $\eta_s = 1$ and $\eta_p = \eta_{p0}$. Once the polymer has lost its elastic energy related to intramolecular bonds and long-range repulsion, the free energy decreases with an increase of η_p owing to growth of configurational entropy, which paves the way for spontaneous unfolding. The unfolded random coil is then vulnerable to irreversible transformations such as aggregation or refolding to amyloid structure (17).

The transition rate along the reaction coordinate η_s is calculated $k(T) = A\exp(-\Delta G/RT)$, with $\Delta G(T) = G(\eta_{p0}, 1, T) - G_0$, where $G(\eta_{p0}, 1, T) = -a^2(T - T_m)T/2B + |\Delta S_{solv}|T$ and G_0 could be neglected as a second-order term in $(T - T_m)/T$. The dependence of transition rate on temperature is found to be

$$k(T) = \mathrm{A}\ \exp(-|\Delta S_{solv}|\ /\ \mathrm{R})\ \exp\left(a^2(T - T_m)\ /\ (2BR)\right)$$

and in more convenient notation,

$$k(T)/k(T_m) = \exp((T - T_m)\ln(U)) = U^{(T - T_m)}$$

where $\ln(U) \equiv a^2/(2BR)$ with dimensions of 1/K.

We stress that the temperature dependence of the inactivation rate could follow $k \propto exp(S(T)/R)$, as suggested by Zwanzig (24), in contrast to the more familiar Arrhenius form. A demonstration of such a case appears in Fig. 1, based on interpretation of the simulation found in (19) for the globule and molten globule states. Calculation of the energies $E1 = E(\eta_{p0}(T))$ and $G1 = E1 - S1 \times T = G_0(T)$ is made according to the minimal point in free energy (η_{p0}, G_0) in the case $\eta_s = 0$ as described above. We assume that the melting of a globule occurs at temperature 37°C (transition between points p1 and p2), whereas the polymer remains as a molten globule between points p2 and p3. The transition to random coil requires that the polymer be wetted, for which an entropy barrier of negative ΔS must be surmounted. On the other hand, the energy E2 is independent of temperature after removal of the elastic energy associated with $\eta_{p0}(T)$. Altogether, the free energy barrier $\Delta G = G_2 - G_1$ for the transition from molten globule to random coil state is smaller by 12 kJ/mole at temperature 56°C compared to 37°C. Hence, the former rate is 190 times higher than the latter. Reaching the same rate dependence in an Arrhenius model would require an energy barrier $E_a = 235$ kJ/mole, an order of magnitude larger than the energies considered in this example (see Data S1).

We define the inactivation parameter Ω as the 10-base logarithmic reduction in the number of active virus copies, $\Omega = \log_{10}(N(0)\ /N(t))$. Expecting a memoryless stochastic process, the number of copies should decay exponentially with time; hence, the required exposure time should scale as $t_\Omega(T) = \Omega \times t_1(T)$. The subscript denotes inactivation parameter; for example, t_1 is time to achieve 1 log decay. A tradeoff between temperature and exposure time $t_\Omega(T)$ is described in the relation $\Omega = k(T)t_\Omega(T)/\ln(10)$. Hence, with the aforementioned inactivation rate $k(T) = \tilde{A}U^{(T-T_m)}$ the calculation of exposure time as function of temperature and inactivation parameter is readily achieved: $t_\Omega(T) = (ln10\ /\tilde{A})\Omega U^{(T_m - T)}$. Owing to the multiplicity of protein copies in the virus, we should expect that the factor $1/\tilde{A}$ is increased by a redundancy factor compared to the denaturation time for a single protein.

RESULTS AND DISCUSSION

Our model proposes an activation free energy of the form $\Delta G = -\Delta E_{(T-T_m)} + |\Delta S_{solv}|T$, in contrast to the constant activation energy $\Delta G = E_a$ assumed in the classical Arrhenius model. Because the inactivation rate follows $k = A\exp(-\Delta G/RT)$, the plot of ln(k) vs. 1/T reflects the linear dependence of $\Delta E_{(T-T_m)}/T$ on $(T - T_m)$, predicted based on the Landau theory analysis. According to (29), most of the measured ΔG is due to hydrophobic solvation, and assuming its form $|\Delta S_{solv}|T$, this part does not contribute to the slope in Arrhenius fit. The supposed globule melting stage may explain the suppression of energy barrier E_a. Yet, even if the process involves an energy barrier, the contribution of E_a/T to the Arrhenius slope is smaller by an order of magnitude compared to the contribution of $\Delta E_{(T-T_m)}/T$. Measurements of single proteins in atomic force spectroscopy show that the typical part of entropy-related recoiling energy (the temperature dependent part) in the total free energy of unfolding is 9–14% (23,29), which means that E_a could not dominate the Arrhenius slope. Therefore, the

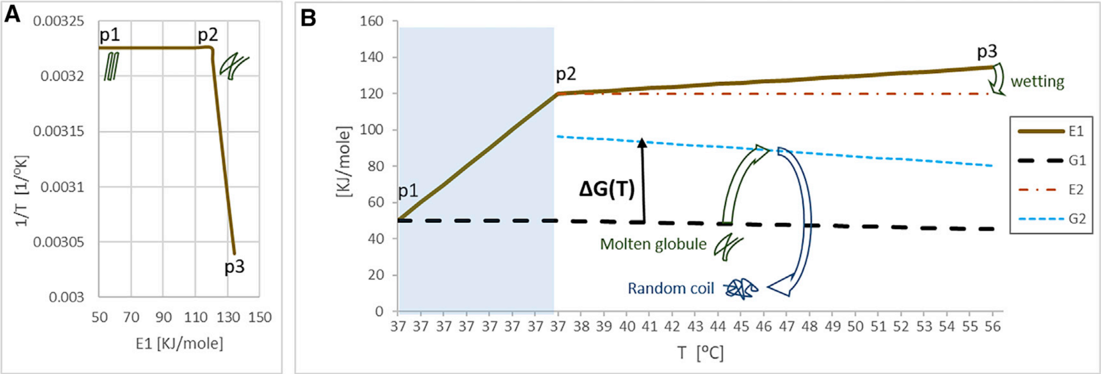

FIGURE 1 (A) Demonstration of transition from globule to molten globule based on a result in (19) and calculations in the text. The transition from point p1 to p2 is a first-order transition in which the free energy remains unchanged. The change in interaction energy of the molten globule between p2 and p3 is approximately balanced with entropy and is calculated according to Landau's theory of second-order phase transition. (B) The globule to coil transition rate increases with temperature owing to decrease in the barrier $\Delta G = G2 - G1$. The energy E1 and free energy G1 refer to the globule or molten globule state. The gray area represents a coexistence region. The E2 and G2 plots refer to the critical intermediate state of transition from molten globule to coil, which involves wetting of the polymer and overcoming a solvation entropy barrier $|\Delta S| = 150$ J/mol/K. Wetting removes the variation of E2 with temperature and reduces the system entropy as $S2 = -|\Delta S| + S1$. The variation of entropy with temperature is calculated according to Landau's theory $S1(T) = S(p2) + 2.37$ $[J/mol/K^2] \times (T - T_m)$, fitted with the ratio of inactivation rates of SARS-CoV-2 between 37 and 56°C. ΔG appears approximately linear with $T - T_m$ because the trivial dependence on a factor T is negligible. To see this figure in color, go online.

major temperature dependence in the transition rate emerges from $\Delta E_{(T-T_m)}$, and based on the Landau theory analysis, $k(\mathrm{T})$ is proportional to $U^{(T-T_m)}$.

The form of temperature dependence $U^{(T-T_m)}$ coincides with an empirical law of thermal damage to cells established by Sapareto and Dewey (30) and often practiced in hyperthermia medicine (31). According to Sapareto and Dewey (30), the rate of heat damage in cells follows $U^{(T\ -\ 43^{\circ}\mathrm{C})}$, with T in Celsius units, where the value $r = 1/U$ is between 0.4 and 0.8 for $T > 43^{\circ}\mathrm{C}$ (0.5 being the most common number), and is around $r = 0.25$ for $T < 43^{\circ}\mathrm{C}$. The justification for a split temperature range is the onset of thermotolerance in living cells (31). In the case of virus inactivation, a single range seems adequate.

The important finding of (9,10) is that for various types of coronaviruses, the inactivation rate $\ln(k)$ is approximately linear with reciprocal temperature 1/T, similar both to classical Arrhenius law and to the proposed model. Despite the difference in the underlying mechanism, it is shown below that the proposed model and the classical Arrhenius model with constant activation energy agree in mathematical description up to first order in $|T - T_m|/T_m$, which is below 0.1.

Based on Taylor's expansion

$$\frac{1}{T} \approx \frac{1}{T_m} + \frac{\partial\left(\frac{1}{T}\right)}{\partial T}(T - T_m) = \frac{1}{T_m} - \frac{1}{T_m^2}(T - T_m),$$

with neglect of higher-order terms,

$$k(T) = A\exp\left(-\frac{E}{RT}\right) \approx \tilde{A}U^{(T-T_m)}$$

where $U = \exp\left(\frac{E}{R{T_m}^2}\right)$ and $\tilde{A} = A\exp\left(-\frac{E}{RT_m}\right)$.

Therefore, knowledge of the transition temperature T_m, at least approximately, allows extracting meaningful values from the A and E parameters in the Arrhenius fit: U is related to Landau's parameters and $\tilde{A}$ is the native reaction rate. As noted in (15), results of membrane protein inactivation fitted to Arrhenius model often yield E in a range between 2.0 and $3.0 \times 10^5\ \mathrm{Jmol}^{-1}$, whereas in (9), E is between 0.8×10^5 and $2.2 \times 10^5\ \mathrm{Jmol}^{-1}$. We can fit the same data referenced in that work to our model. In Kelvin units, using $R = 8.314\ \mathrm{J} \times \mathrm{K}^{-1}\ \mathrm{mol}^{-1}$, $T_m = 310$ K, we find for the range of general inactivation that U lies between 1.28 and 1.46, whereas the value of U among coronaviruses is between 1.10 and 1.31. Based on the Arrhenius fitting parameters A and E for coronaviruses found in (10) and $T_m = 310$ K, we find that the range of $\tilde{A}$ (present model) is between 0.005 and 0.050 min^{-1}, in contrast to the unphysically large range of the attempt frequencies A (see Table 1; Data S1). In practice, the discrepancy between predictions of the energy barrier and free energy barrier models is minor compared with experimental uncertainty of the data at hand. Other heuristic fitting formulas also provide reasonable agreement with the limited data (8–10). However, the underlying physical models are very different and with further development could provide a key, for example, to evaluate the risk of possible mutations in the virus.

TABLE 2 SARS-CoV-2 data

Medium	Ω, $\log_{10}$ reduction	T, Temperature	t_Ω, Exposure time
Sputum	4 ± 1	37°C	48 h
Sputum	6 ± 1	42°C	24 h
Sputum	4	56°C	15 min

Relevance to SARS-CoV-2 inactivation by fever

We focus our attention on temperatures near physiological, which are relevant to fighting the virus inside the body.

Measurements on thermal inactivation of SARS-CoV-2 are found in (5), performed by a group of FDA researchers on sputum samples spiked with the virus. Table 2 shows the reduction in viral infectivity after exposure to different temperatures.

In (14), SARS-CoV-2 inactivation was tested in cell culture and in human serum by a team experienced with similar measurements in MERS-CoV. The relevant values are shown in Table 3.

For comparison, we show in Table 4 data on SARS-CoV-1 obtained from (32) based on tests in various hospitals. Evidently, SARS-CoV-2 is inactivated more rapidly than SARS-CoV-1.

The uncertainty in measurements of the $\log_{10}$ reduction is expected to be around 1 log unit, so the expressed uncertainty in inactivation rate is ~30% or 0.15 in log scale. The data points are shown in Fig. 2, fitted with the Arrhenius model and our power-law model. The latter is fitted with two points compared with three in the Arrhenius model, which make the slight difference in the curves. (5) provides evidence of temporary increase in the number of copies in the samples, suggesting unaccounted replication at some stage of the test. (14) reports only a monotonic decrease

TABLE 1 Range of parameters for different coronaviruses in arrhenius model compared with the proposed model

Source	Arrhenius: A, attempt rate [1/min]	Arrhenius: E, activation energy [kJ/mole]	Proposed $\tilde{A}$, native reaction rate [1/min]	Proposed U, scaling parameter [exp(1/K)]
(9)	10^{10}–10^{35}	77–217	0.001–0.064	1.10–1.31
(10)	10^{15}–10^{30}	100–195	0.005–0.050	1.13–1.28

TABLE 3 SARS-CoV-2 data

Medium	Ω, $\log_{10}$ reduction	T, Temperature	t_Ω, Exposure time
Cell culture	3.4	56°C	15 min
Serum	3.6	56°C	10 min

TABLE 4 SARS-CoV-1 data

Medium	Ω, $\log_{10}$ reduction	T, Temperature	t_Ω, Exposure time
Suspension	4	60°C	30 min
Suspension	4	65°C	15 min

in population; however, the rate of decrease is smaller in cell culture than in serum. These aspects of the data remain unclarified but basically introduce an uncertainty in the measurement.

The working values for inactivation of SARS-CoV-2 are 48 h at 37°C and 15 min at 56°C. Both conditions achieve 99.99% (4 $\log_{10}$) reduction in infectivity. According to the model, $(48 \times 60\text{min}/15\text{min}) = (t_4(37^0\text{C})/t_4(56^0\text{C})) = U^{(56-37)}$, and hence U = 1.32, which is among the highest values compared to Table 1. The native reaction rate is $\tilde{A} = 0.0032\ \text{min}^{-1}$.

The estimate of exposure time at temperature T in Celsius to achieve inactivation parameter 4 (4 $\log_{10}$ reduction) is thus

$$t_4(T) = 1.32^{\left(37^0\text{C}-T\right)} \times 48\ \text{h}$$

Applying the calculation, a moderate fever of 39°C for 28 h should achieve 99.99% inactivation of the SARS-CoV-2 virus; 14 h is expected to reach 99% inactivation.

As a control, we check that $t_{6\,\pm\,1}(42°\text{C}) = ((6 \pm 1)/4)\ t_4(42°\text{C}) = 18 \pm 3$ h, which agrees reasonably well with the measured value around 24 ± 5 h. Notably, our predictions do not rely on a particular theory because the model is satisfied empirically in multiple cases of virus inactivation.

CONCLUSIONS

We expect that thermal inactivation of SARS-CoV-2 involves wetting by water in combination with variation in conformational entropy of part of a protein due to a second-order phase transition to an unfolded or ineffectually folded state. In this case, the suggested formula to extrapolate thermal inactivation time at temperature T and inactivation parameter Ω from a known time of exposure and inactivation parameter $t_{\Omega 1}(T1)$ at temperature $T1$ is

$$t_\Omega(T) = t_{\Omega 1}(T1)U^{(T1-T)}\Omega/\Omega 1$$

U can be determined from measurements at two temperature points,

$$U = \left[(\Omega 1/\Omega 2) \times t_{\Omega 2}(T2)/t_{\Omega 1}(T1)\right]^{1/(T1-T2)}$$

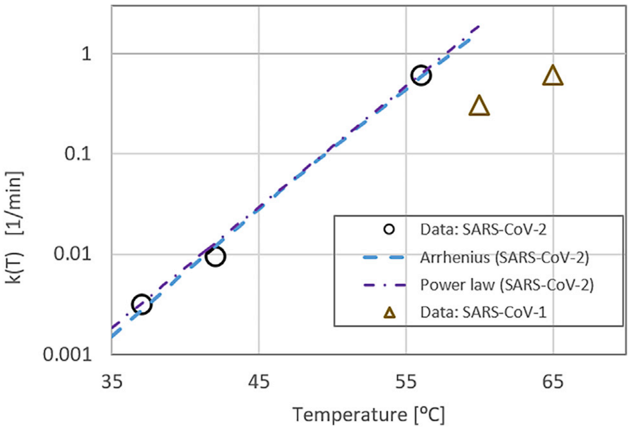

FIGURE 2 Inactivation rate as a function of temperature for SARS-CoV-2 and SARS-CoV-1. The former is fitted with the Arrhenius model using linear regression of three points, ln(k) = 86.8–239[KJ]/R(T + 273), and the power law is fitted using two points as shown in the text: ln(k) = ln(k(37)) + (T − 37°C)ln(1.32). To see this figure in color, go online.

For SARS-CoV-2, U = 1.32, and the results show a clear benefit to moderate fever in fighting the virus. At body temperature of 39°C, we expect inactivation of 99% after 14 h and inactivation of 99.99% after 28 h.

The proposed model differs fundamentally from the more common fitting to an Arrhenius behavior with a constant energy of activation and a prefactor relating to the attempt frequency. Given the limited temperature range for the available data, it is not possible to choose between models solely on the basis of the scaling fit quality. Therefore, our interpolations regarding the virus inactivation rates are equally well supported by the conventional model. However, one can look to the range of parameters required in making the fit. Given the basic similarity of proteins as organic polymers, as well as the common architecture of coronaviruses, one would not expect a difference of many orders of magnitude in parameters describing the kinetics of inactivation among different examples. At the very least, such parameters must be divorced from their conventional physical interpretations. By contrast, we find that the entropy-related model is satisfied with stable parameters.

A visit to the sauna has been suggested as treatment for Covid-19 patients (33), based on the prediction that the air temperatures may reach 85°C and the temperature in the trachea could reach up to 45°C despite the body perfusion (34). According to our model, however, $t_4(45°\text{C}) = 7$ h would be required to achieve 4 log10 damage, whereas the recommended time in sauna is ~15 min. The intact fraction of the virus after 15 min is $10^{-4\,\times\,0.25/7}$, which is 70%, so a visit to sauna may extinguish up to 30% of the SARS-CoV-2 viruses in the lower respiratory tract. The sauna may have other benefits, and it is not a likely locale for transmission. Perhaps it could prevent illness at early stages of infection in the nasal region, but simple thermal inactivation in the lower airways of an infected individual is not likely.

One explanation for the good coping of young children with Covid-19 is their rapid fever response to infection (35). The possibility of increasing core body temperature is still being investigated (1), yet the recommendation to avoid antipyretic agents in cases of moderate fever seems justified.

SUPPORTING MATERIAL

Supporting Material can be found online at https://doi.org/10.1016/j.bpj.2020.11.2259.

AUTHOR CONTRIBUTIONS

S.S. and M.E. performed the research and wrote the article. S.S. handled the calculations.

ACKNOWLEDGMENTS

M.E. is an incumbent of the Sam and Ayala Zacks Professorial Chair. The lab has benefited from the historical generosity of the Harold Perlman family.

REFERENCES

1. Mercado-Montoya, M., N. Bonfanti, …, E. Kulstad. 2020. The use of core warming as a treatment for coronavirus disease 2019 (COVID-19): an initial mathematical model. *J. Card. Arrhythm.* 33:6–15.
2. Schell-Chaple, H. M., K. A. Puntillo, …, K. D. Liu; National Heart, Lung, and Blood Institute Acute Respiratory Distress Syndrome Network. 2015. Body temperature and mortality in patients with acute respiratory distress syndrome. *Am. J. Crit. Care.* 24:15–23.
3. Darnell, M. E. R., K. Subbarao, …, D. R. Taylor. 2004. Inactivation of the coronavirus that induces severe acute respiratory syndrome, SARS-CoV. *J. Virol. Methods.* 121:85–91.
4. Lee, Y.-N., L.-K. Chen, …, S.-Y. Lo. 2005. Thermal aggregation of SARS-CoV membrane protein. *J. Virol. Methods.* 129:152–161.
5. Wang, T., C. Lien, …, P. Selveraj. 2020. Effective heat inactivation of SARS-CoV-2. *medRxiv* https://doi.org/10.1101/2020.04.29.20085498.
6. Wang, Y., X. Wu, …, Y. Luo. 2004. Low stability of nucleocapsid protein in SARS virus. *Biochemistry.* 43:11103–11108.
7. Abraham, J. P., B. D. Plourde, and L. Cheng. 2020. Using heat to kill SARS-CoV-2. *Rev. Med. Virol.* 30:e2115.
8. Guillier, L., S. Martin-Latil, …, M. Sanaa; Covid-19 Emergency Collective Expert Appraisal Group. 2020. Modeling the inactivation of viruses from the *Coronaviridae* family in response to temperature and relative humidity in suspensions or on surfaces. *Appl. Environ. Microbiol.* 86:e01244-20.
9. Yap, T. F., Z. Liu, …, D. J. Preston. 2020. A predictive model of the temperature-dependent inactivation of coronaviruses. *Appl. Phys. Lett.* 117:060601.
10. Hessling, M., K. Hoenes, and C. Lingenfelder. 2020. Selection of parameters for thermal coronavirus inactivation - a data-based recommendation. *GMS Hyg. Infect. Control.* 15:Doc16.
11. Doniach, S., T. Garel, and H. Orland. 1996. Phase diagram of a semiflexible polymer chain in a θ solvent: application to protein folding. *J. Chem. Phys.* 105:1601–1608.
12. Ziv, G., D. Thirumalai, and G. Haran. 2009. Collapse transition in proteins. *Phys. Chem. Chem. Phys.* 11:83–93.
13. Kolinski, A., J. Skolnick, and R. Yaris. 1986. Monte Carlo simulations on an equilibrium globular protein folding model. *Proc. Natl. Acad. Sci. USA.* 83:7267–7271.
14. Batéjat, C., Q. Grassin, …, I. Leclercq. 2020. Heat inactivation of the severe acute respiratory syndrome coronavirus 2. *bioRxiv* https://doi.org/10.1101/2020.05.01.067769.
15. Roman, E. A., and F. L. González Flecha. 2014. Kinetics and thermodynamics of membrane protein folding. *Biomolecules.* 4:354–373.
16. Cattoni, D. I., F. L. González Flecha, and J. M. Argüello. 2008. Thermal stability of CopA, a polytopic membrane protein from the hyperthermophile Archaeoglobus fulgidus. *Arch. Biochem. Biophys.* 471:198–206.
17. Borzova, V. A., K. A. Markossian, …, B. I. Kurganov. 2016. Kinetics of thermal denaturation and aggregation of bovine serum albumin. *PLoS One.* 11:e0153495.
18. Wrapp, D., N. Wang, …, J. S. McLellan. 2020. Cryo-EM structure of the 2019-nCoV spike in the prefusion conformation. *Science.* 367:1260–1263.
19. Maffi, C., M. Baiesi, …, P. De Los Rios. 2012. First-order coil-globule transition driven by vibrational entropy. *Nat. Commun.* 3:1065.
20. Rubinstein, M., and R. H. Colby. 2003. Polymer Physics. Oxford University Press, Oxford, UK.
21. Imandi, V., and A. Chatterjee. 2016. Estimating Arrhenius parameters using temperature programmed molecular dynamics. *J. Chem. Phys.* 145:034104.
22. Zwanzig, R. 1995. Simple model of protein folding kinetics. *Proc. Natl. Acad. Sci. USA.* 92:9801–9804.
23. Carrion-Vazquez, M., A. F. Oberhauser, …, J. M. Fernandez. 1999. Mechanical and chemical unfolding of a single protein: a comparison. *Proc. Natl. Acad. Sci. USA.* 96:3694–3699.
24. Zhou, H., and R. Zwanzig. 1991. A rate process with an entropy barrier. *J. Chem. Phys.* 94:6147–6152.
25. Vidugiris, G. J. A., J. L. Markley, and C. A. Royer. 1995. Evidence for a molten globule-like transition state in protein folding from determination of activation volumes. *Biochemistry.* 34:4909–4912.
26. Haran, G. 2012. How, when and why proteins collapse: the relation to folding. *Curr. Opin. Struct. Biol.* 22:14–20.
27. Landau, L. D., and E. M. Lifshitz. 1980. Chapter XIV - Phase transitions of the second kind and critical phenomena. *In* Statistical Physics, Third Edition. L. D. Landau and E. M. Lifshitz, eds. Butterworth-Heinemann, pp. 446–516.
28. Ball, P. 2008. Water as an active constituent in cell biology. *Chem. Rev.* 108:74–108.
29. Walther, K. A., F. Gräter, …, J. M. Fernandez. 2007. Signatures of hydrophobic collapse in extended proteins captured with force spectroscopy. *Proc. Natl. Acad. Sci. USA.* 104:7916–7921.
30. Sapareto, S. A., and W. C. Dewey. 1984. Thermal dose determination in cancer therapy. *Int. J. Radiat. Oncol. Biol. Phys.* 10:787–800.
31. Dewhirst, M. W., B. L. Viglianti, …, M. Hanson. 2003. Thermal dose requirement for tissue effect: experimental and clinical findings. *Proc. SPIE Int. Soc. Opt. Eng.* 4954:37.
32. Kampf, G., A. Voss, and S. Scheithauer. 2020. Inactivation of coronaviruses by heat. *J. Hosp. Infect.* 105:348–349.
33. Cohen, M. 2020. Turning up the heat on COVID-19: heat as a therapeutic intervention. *F1000 Res.* 9:292.
34. Soni, B., and A. K. Nayak. 2019. Effect of inspiration cycle and ventilation rate on heat exchange in human respiratory airways. *J. Therm. Biol.* 84:357–367.
35. Barbi, E., P. Marzuillo, …, B. S. Krauss. 2017. Fever in children: pearls and pitfalls. *Children (Basel).* 4:81.